Cu(γ,p)X reaction at $E_\gamma = 150$ and 300 MeV

R. A. Schumacher, G. S. Adams, D. R. Ingham,* J. L. Matthews, W. W. Sapp, and R. S. Turley
Department of Physics and Laboratory for Nuclear Science, Massachusetts Institute of Technology, Cambridge, Massachusetts 02139

R. O. Owens
Department of Natural Philosophy, University of Glasgow, Glasgow, Scotland

B. L. Roberts
Department of Physics, Boston University, Boston, Massachusetts 02215
(Received 19 October 1981)

Inclusive photoproton cross sections for the reaction Cu(γ,p)X have been measured for a photon energy of 300 MeV at proton angles 45°, 90°, and 135°, and for 150 MeV at 45°. The data are compared with an intranuclear-cascade calculation and with Ni($\pi^{\pm}$,p) data. The angular distribution is analyzed to obtain an estimate of the number of nucleons involved in the interaction.

[NUCLEAR REACTIONS Cu(γ,p)X, $E=150$ MeV, $\theta=45°$, $E=300$ MeV, $\theta=45°$, 90°, 135°; measured $\sigma(E_p,\theta)$; intranuclear cascade analysis.]

I. INTRODUCTION

Measurements of photoproton cross sections at intermediate energies are expected to yield information both on nuclear structure and on photonuclear reaction mechanisms. At energies above that of the giant dipole resonance, the photon is presumed to interact predominantly with single nucleons or with few-nucleon systems in the nucleus. The large mismatch between photon and nucleon momentum in the single nucleon absorption process leads to the hypothesis of two-nucleon absorption, in which the photon's energy is shared by two nucleons with small total momentum in the final state, viz., the familiar quasideuteron model. In addition to this mechanism, photons with energies greater than about 150 MeV can interact with a single nucleon through the pion production process ($\gamma+N \rightarrow \pi+N$), the cross section for which exhibits a large peak [the $\Delta(1232)$ resonance] at $E_\gamma \approx 300$ MeV.

Measurements of the cross sections for (γ,p) reactions leading to specific final nuclear states are, in principle, sensitive to the structure of the nuclei involved. In particular, effects such as high momentum components and short range correlations in nuclear ground state wave functions have been discussed.[1] The quantitative interpretation of these data is complicated, however, by uncertainties in the reaction mechanism. Although mesonic exchange currents[2] and virtual $\Delta(1232)$ excitation[3] have both been incorporated into recent calculations, the agreement with the data is still only qualitative.[4]

The (γ,p) cross section resulting in large excitation energies ($\gtrsim 50$ MeV), on the other hand, is not expected to depend on details of nuclear structure. It is hoped, therefore, that measurements of cross sections for these inclusive processes will aid in the elucidation of the reaction mechanism. The cross section in the energy region of the $\Delta(1232)$ resonance is of particular interest. Since the total $\gamma+N$ cross section at $E_\gamma \approx 300$ MeV is dominated by the pion production process, the photon can be viewed as a means of "planting" a Δ in the nuclear interior. By comparison, incident pions, which might be considered a more direct way to produce a Δ, interact mainly in the nuclear surface.[5] Since most of the high energy photoprotons ($E_p = 100-200$ MeV) presumably result from processes in which the pion

is reabsorbed, a measurement of the angular distribution of these protons could provide useful information on the propagation and the decay of the Δ within the nuclear medium.[6]

To date, only phenomenological calculations have been performed for the inclusive (γ,p) cross section $d^2\sigma/dE_p d\Omega_p$. For energies below the pion threshold, the quasideuteron model has been employed.[7] Final state interactions have been included most accurately in the intranuclear cascade calculations of Gabriel and Alsmiller,[8] which include both the quasideuteron and the quasifree pion production processes. This calculation will be discussed further, and compared with the results of the present experiment, in a later section.

Experimental data on inclusive (γ,p) processes in which both the photon and the proton energies are well defined have until quite recently been sparse, due mainly to the difficulties associated with generating a monoenergetic photon beam (or its equivalent through bremsstrahlung subtraction) of sufficient intensity and energy resolution. There are a few measurements of the proton spectra from ^{6}Li (Ref. 9), ^{7}Li, ^{9}Be, and ^{12}C (Ref. 10), for $E_\gamma \approx 100$ MeV. At higher energies early measurements were performed for ^{12}C by Weil and McDaniel[11] ($E_\gamma = 190 \pm 30$ MeV, $\theta_p = 60 \pm 15°$) and by Cence and Moyer[12] ($E_\gamma = 245 \pm 15$ MeV, $\theta_p = 60°$). More recently, this latter measurement has been repeated by Dougan and Stiefler[13] and extended to higher energies[14] ($E_\gamma = 396 \pm 17$ MeV). The proton spectrum for ^{9}Be at $\theta_p = 25° \pm 5°$ has been measured by Homma *et al.*[15] for $E_\gamma = 200-400$ MeV ($\Delta E_\gamma = 20$ MeV).

The most extensive program of inclusive (γ,p) measurements has been carried out at the Bonn 500-MeV synchrotron with the tagged photon beam facility ($E_\gamma = 200-385$ MeV, $\Delta E_\gamma = 10$ MeV). For ^{12}C, photoproton spectra were measured at four angles using a magnetic spectrometer,[16] and compared with the results of the cascade calculation.[8] For eight other nuclei ($A = 4-208$) measurements were performed with somewhat poorer statistics and resolution at five angles simultaneously using an array of time-of-flight spectrometers.[17] In both experiments charged pions were also detected[18]; the aim of the latter experiment was to determine the total hadronic cross section in the Δ(1232) resonance region as a function of A.

The goal of the present experiment was to determine the proton spectrum with good energy resolution and statistics from the inclusive (γ,p) reaction on a medium weight nucleus. The bremsstrahlung difference method, used with the intense bremsstrahlung beam available from the MIT Bates Linear Accelerator, allowed such a measurement at a single equivalent monoenergetic photon energy to be performed relatively quickly. Because of the interest in the Δ region, we selected the energy $E_\gamma = 300$ MeV and performed measurements of the Cu$(\gamma,p)X$ spectra for $E_p = 50-200$ MeV at $\theta_p = 45°$, 90°, and 135°. In addition, we obtained one spectrum for $E_\gamma = 150$ MeV at $\theta_p = 45°$. The choice of target nucleus was motivated by the existence of proton spectra from the Ni$(\pi^\pm,p)$ reaction[19] at $E_\pi = 160$ MeV with which our results could be compared.

II. EXPERIMENTAL ARRANGEMENT

Bremsstrahlung photons were produced by an electron beam incident on a 249 mg/cm^2 (0.05 radiation length) tungsten radiator. A target of natural copper (either 113 mg/cm^2 or 284 mg/cm^2) was situated 10 cm from the radiator so that it intercepted the entire bremsstrahlung flux. Data for each proton energy were taken in pairs of runs with the electron energy varied by 10 MeV such that the peak of the difference between the corresponding bremsstrahlung spectra was centered at 300 or 150 MeV. The difference method used to obtain effectively monochromatic photons will be described in detail in Sec. III. The full width at half maximum of the effective photon spectrum was about 12 MeV.

The protons were momentum analyzed with the 900 MeV/c spectrometer.[20] The solid-angular acceptance of the spectrometer was defined by a pair of slits, and was typically 1.6 msr in this experiment. The focal plane instrumentation consisted of multiwire chambers with delay line readouts in both the momentum and the scattering angle planes, and a set of five trigger counters. These counters were constructed from NE110 plastic scintillator sheets of thicknesses 1.6, 2.3, 3.1, 12.5, and 12.5 mm coupled to RCA 8575 phototubes as described in Ref. 21. Depending on the proton energy, a coincidence between two to five counters was required to trigger the wire chamber readouts.

The electronics consisted of standard fast NIM and CAMAC instrumentation. For each event detected by the trigger counters the pulse height in each of the plastic scintillators and the arrival time of the pulses at each end of the wire chamber delay lines were read into a PDP 11/45 computer. An

on-line calculation determined and recorded the location of each event on the focal plane.

III. BREMSSTRAHLUNG DIFFERENCE TECHNIQUE

In this experiment, data for each proton energy were taken at two electron beam energies separated by 10 MeV. The difference between these proton yields is essentially the contribution to the cross section due to photons produced in the energy region between the endpoints of the two bremsstrahlung curves. Let $\sigma_\gamma \equiv d^2\sigma/d\Omega_p\, dE_p$ represent the photoproton cross section being measured. The measured yield of protons at a fixed proton energy E_p will be a convolution of the cross section σ_γ with the photon spectrum:

$$N_p = G \int \sigma_\gamma \left[N_e \frac{dn_\gamma}{dE_\gamma} \right] dE_\gamma ,$$

where the integral is taken over the kinematically allowed photon energy range, and G is a geometrical factor containing the target thickness, spectrometer solid angle, energy bite, and constants. Here $N_e(dn_\gamma/dE_\gamma)$ represents the number of photons per unit energy, where N_e is the number of incident electrons and dn_γ/dE_γ is the photon yield per electron. If two runs (a) and (b) are taken with endpoint energies E_a and E_b then the proton yields can be subtracted, after normalization by a factor C, to give:

$$\frac{N_p^{(a)}}{N_e^{(a)}} - C\frac{N_p^{(b)}}{N_e^{(b)}} = G\sigma_\gamma \int \left[\frac{dn_\gamma^{(a)}}{dE_\gamma} - C\frac{dn_\gamma^{(b)}}{dE_\gamma} \right] dE_\gamma . \tag{1}$$

The constant C is selected so as to minimize the low energy tail of the difference spectrum whose contribution to the integral is then neglected. It is assumed that σ_γ is constant over the peak region of the photon difference spectrum and is thus determined by the difference between two measured proton yields, for which the corresponding bremsstrahlung difference flux can be calculated.

The electrodisintegration contribution to the proton yield, which is present since both electron and bremsstrahlung beams pass through the target, can be accounted for in two ways. One method is to measure it directly by doing a radiator-out run for each proton energy and subtracting this contribution from the radiator-in data. This correction is not exact since it takes no account of the straggling of the electron energy spectrum in the radiator; it also doubles the required running time. Alternatively, one can adopt the virtual photon approach in which after some approximations the electrodisintegration cross section can be written as an integral over photon energy of the product of the real photon cross section and a calculable virtual photon spectrum. The terms dn_γ/dE_γ in Eq. (1) are then replaced by the total photon spectrum, i.e., the sum of the bremsstrahlung and the virtual photon spectra. The constant C is then chosen to minimize the low energy tail of the total difference spectrum. In order to obtain a result with the smallest statistical error the second method was used in this experiment but the validity of the procedure was checked by the first method at several points as explained below.

The calculated photon intensity spectrum included bremsstrahlung from the radiator taking account of the energy spread of the incident electrons and the electron energy loss straggling due to radiative and collisional processes, bremsstrahlung from the target without account of further straggling, and the effective virtual photon contribution in the target. The calculations for the real photon contributions followed Ref. 22 and the virtual spectrum contribution was obtained from the formulas given by Dalitz and Yennie[23] with a first order correction for finite nuclear size[24] applied in the endpoint region. Figure 1 shows the 300-MeV total photon difference spectrum for the tungsten radiator, the 113 mg/cm^2 copper target, and beam energies of 307 and 297 MeV. The low energy tail of this distribution has been minimized by multiplying the 297 MeV endpoint spectrum by 1.006 before subtraction. The contributions from the radiator, target, and virtual photon spectra were 68, 11, and 21 percent of the total, respectively. For the similar 150 MeV case using beam energies of 147 and 157 MeV the contributions of radiator, target, and the virtual photon spectra were 66, 11, and 23 percent, respectively, and the multiplying factor was 1.016.

The most uncertain part of the calculated photon spectrum was the virtual photon component. To test the virtual photon calculation radiator-out data were taken at several widely spaced proton energies. For these runs the electroproduction contribution was dominant compared to bremsstrahlung from the target. The total difference spectrum was calculated for these radiator-out runs and the cross section σ_γ was extracted by the same method used for the radiator-in runs [Eq. (1)]. In all cases the resulting cross sections from radiator-out runs were

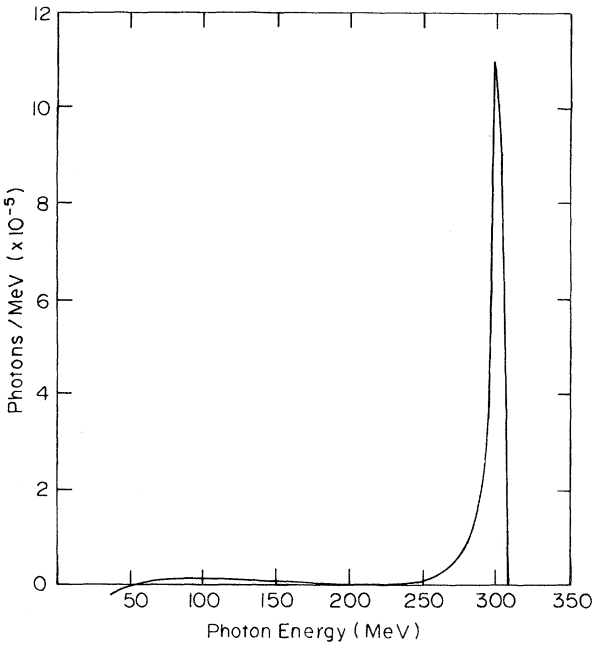

FIG. 1. The difference of two total photon spectra with endpoints at 307 and 297 MeV resulting in an effective spectrum of photons centered at 300 MeV with a full width of about 12 MeV. The intensity in the region below the peak was minimized by weighting the 297 MeV spectrum by a factor of 1.006.

within one standard deviation of the results obtained with the radiator in. This indicates that the treatment of the electrodisintegration contribution in terms of the virtual photon approximation is adequate for the present purpose.

As a typical result of the calculations outlined above, the total yield for a 0.05 radiation length tungsten radiator and a 113 mg/cm^2 copper target is $(1.40\pm0.08)\times10^{-3}$ photons per electron in the peak of the difference spectrum. The accuracy of this result is estimated to be $\pm4\%$ for the bremsstrahlung contribution and $\pm20\%$ for the electrodisintegration contribution, leading to a weighted overall accuracy of $\pm6\%$.

IV. EXPERIMENTAL DATA

A. Data taking procedure

The measurements covered the proton spectrum in 5% steps in momentum. Runs corresponding to the two halves of each difference measurement were taken consecutively and repeated several times. This reproducibility check was necessary since the differences were in some instances as small as 5%. Radiator-out data were taken at a representative sample of the proton momenta, as explained in Sec. III. The background rate due to the radiator and other sources was measured occasionally by doing target-out runs and was always found to be $\leq0.6\%$ of the total event rate, and nearly independent of E_e.

B. Treatment of the data

The first step in the analysis of the event-by-event data was the generation of correlated pulse height spectra for the purpose of particle identification. Separation of protons from deuterons and other more highly ionizing particles, as well as from the small minimum ionizing background, was always unambiguous using the pulse height information from the scintillators and the position information from the wire chambers; typical energy loss spectra for this experiment are shown in Ref. 21.

The momentum calibration and dispersion of the magnetic spectrometer were determined from inelastic electron scattering measurements at known beam energies. Since the momentum of the protons measured in this experiment exceeded the available electron momentum, the calibration was extended as described in Ref. 25 using protons of calculable momentum at the endpoint of the $^{16}O(\gamma,p)^{15}N$ spectrum. The uncertainty in the spectrometer calibration produces an uncertainty of about 1% in both the calculated mean proton energies and in the cross section values.

Corrections were made to the measured proton yields for two further effects. Events were processed and stored in the computer at a maximum rate of one per beam burst, and only the total number of additional event triggers was recorded. The correction made for this loss was at most 20% with an uncertainty of the order of 0.1%. The drift chamber had a clutter time of about 300 ns, and if additional real or background events occurred within this time the initial event was rejected. Corrections for this loss were at most 3%.

The errors listed above together with estimated uncertainties in the target and radiator thicknesses, spectrometer solid angle, and integrated beam current gave a net systematic uncertainty of $\pm3.5\%$, to which must be added the $\pm6\%$ uncertainty in the photon difference spectrum.

C. Results

Figure 2 and Table I show the results of our measurement of the inclusive photoproton cross section

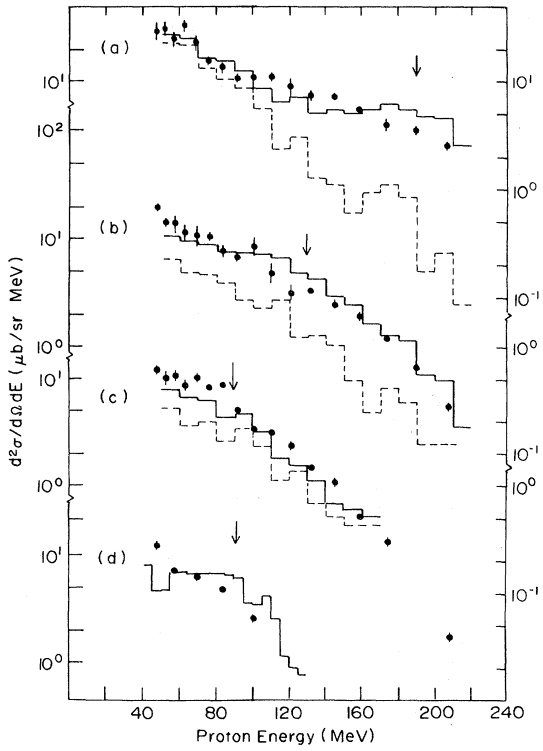

FIG. 2. Cu(γ,p)X cross sections: (a) 300 MeV, 45°; (b) 300 MeV, 90°; (c) 300 MeV, 135°; (d) 150 MeV, 45°. Only statistical errors are shown. Also plotted are the results of a cascade calculation where the solid lines represent the total yield, and the dashed lines the yield due to quasifree pion production only. The arrows indicate the proton energies expected for free deuteron photodisintegration kinematics.

for natural copper as a function of proton energy for θ_p=45°, 90°, and 135° at E_γ=300 MeV and for θ_p=45° at E_γ=150 MeV. Only statistical error bars are shown. The overall systematic uncertainty is ±7%. The data are presented at energy intervals corresponding to $\Delta p/p$=6%, as no fine structure was observed within the 6% momentum acceptance of the spectrometer. The cross sections decrease monotonically with increasing proton energy, and have a maximum value between 10 and 30 μb/sr MeV. Figure 3 shows a comparison of the present 300 MeV, 45° data with recent results from the Bonn tagged photon facility,[26] where the Cu(γ,p)X spectrum was measured at E_γ=291±15 MeV and θ_p=44°. The agreement in the magnitude and shape of the two measurements is reasonably good.

V. DISCUSSION OF RESULTS

A. Reaction mechanisms

The proton spectra observed in recent studies of the (γ,p) reaction on ^{9}Be (Ref. 15) and ^{12}C (Ref. 16) have been interpreted in terms of quasifree pion production and two-nucleon (quasideuteron) absorption processes; the low proton energy region is due mainly to the former process and the high energy shoulder to the latter. However, this distinction is somewhat artificial in the resonance region, where the two processes can more accurately be classed as different decay channels for the Δ whose excitation largely dominates photoabsorption. We note that the present data for Cu(γ,p) show little or no evidence for a shoulder in the region corresponding to two-nucleon absorption. This increased "smearing" of the π production and two-nucleon regions as A increases is presumably a reflection of the increasing importance of final-state interactions.

Included in Fig. 2 are the results of an intranuclear cascade calculation[8,27] for the Cu(γ,p)X reaction. The charge density of the nucleus was modeled by three concentric spheres of uniform density, with the density in each sphere equal to the average of the corresponding continuous charge density. Within each sphere the Fermi momentum distribution for the nucleons was normalized to the number of nucleons in that sphere. The model allowed for pion production and quasideuteron absorption as initial reactions and the calculations followed all secondary particles through the nucleus until they were emitted or absorbed. However, Δ propagation through the nucleus was not included. The strength of the quasideuteron contribution was characterized by an empirical number, L, which relates the effective quasideuteron cross section to the free deuteron cross section multiplied by the number of neutron-proton pairs in the nucleus, i.e., $\sigma_{qd}=(LNZ/A)\sigma_d$. The constant L was not changed from earlier determinations.[8] The solid histograms in Fig. 2 represent the total predicted yield while the dashed histograms indicate the yield from pion production only. It is seen that this latter contribution becomes increasingly important as the proton angle increases, a result, presumably, of pion reabsorption processes. The approximations inherent in an intranuclear cascade calculation make a detailed comparison with experimental data inappropriate; however, the generally good agreement shown in Fig. 2 does suggest that the calculation has accounted satisfactorily for the dominant photoreaction processes.

TABLE I. Inclusive cross sections for the Cu(γ,p)X reaction. Errors given are statistical only. The overall systematic uncertainty is ±7%.

θ_p / E_p (MeV)	E_γ=300 MeV 45° (μb/sr MeV)	E_γ=300 MeV 90° (μb/sr MeV)	E_γ=300 MeV 135° (μb/sr MeV)	E_γ=150 MeV 45° (μb/sr MeV)
47.0	29.0±6.0	19.8 ±1.6	11.6 ±0.9	12.4±1.3
51.7	30.0±4.0	14.0 ±1.2	9.8 ±1.4	
56.9	25.0±4.0	14.0 ±2.7	10.5 ±1.1	7.2±0.5
62.5	33.0±4.0	11.6 ±1.8	8.4 ±0.8	
68.7	23.0±4.0	10.8 ±2.2	9.9 ±1.0	6.2±0.4
75.5	15.5±1.6	10.4 ±0.9	8.0 ±0.5	
82.9	13.7±1.8	7.7 ±1.0	8.5 ±0.5	4.9±0.3
91.0	10.7±1.1	6.8 ±0.6	5.06 ±0.26	
99.9	11.2±1.9	8.6 ±1.8	3.31 ±0.19	2.5±0.18
109.6	11.0±0.6	4.9 ±1.1	3.04 ±0.23	
120.2	8.9±1.9	3.1 ±0.8	2.28 ±0.18	
131.8	7.4±0.9	3.3 ±0.2	1.42 ±0.07	
144.4	7.1±0.6	2.4 ±0.2	1.04 ±0.09	
158.1	5.5±0.3	1.90±0.16	0.51 ±0.03	
173.0	4.0±0.6	1.19±0.07	0.288±0.018	
189.3	3.4±0.3	0.65±0.04		
206.9	2.5±0.2	0.27±0.02	0.039±0.003	

It should perhaps be noted that a cascade calculation by Ginocchio[5,28] for pion-induced reactions, which agrees reasonably well with recent ($\pi^\pm$,p) data[19] in the resonance region, does include incoherent Δ propagation. It is not clear how much significance should be attached to the inclusion of Δ propagation in the successful treatment of ($\pi^\pm$,p) reactions and its absence in equally satisfactory (γ,p) calculations, since Ginocchio does not assess its effect on his results and the two calculations have not been applied to a common reaction.

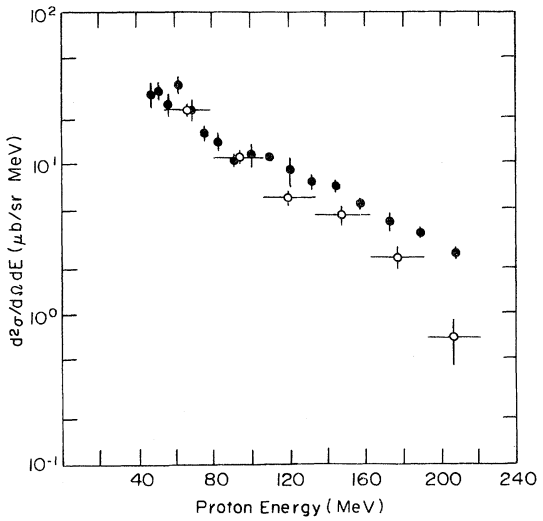

FIG. 3. Comparison of the present data at 300 MeV, 45° (closed circles) with Bonn Cu(γ,p)X data (Ref. 26) for E_γ=291 MeV, 44° (open circles).

B. Analysis of angular distribution

In both the (γ,p) and (π,p) processes further insight into the reaction mechanism would be gained if the number of particles which take part in the interaction between the probe and the nucleus could be determined.[29] If it is assumed that the proton production cross section is isotropic in the reference frame defined by the center of momentum of the incident photon (or pion) and the group of particles in the nucleus which participate in the reaction, then the velocity β of this group of particles can be determined from the forward peaking of the proton energy spectra in the laboratory frame.

Protons which had the same momentum P in the (presumed isotropic) emission frame can be identified by locating points in the proton energy spectra (at each laboratory angle) at which the Lorentz-invariant cross section $(1/cp)(d^2\sigma/dE_p d\Omega_p)$ has the same value. These protons should have momentum

components (in the laboratory) perpendicular and parallel to the incident photon direction which are related to P by

$$p_\perp{}^2+(P^2+m^2c^2)\tanh^2(y_{||}-y)=P^2\ , \qquad (2)$$

where

$$y_{||}=\tanh^{-1}\beta_{||}$$
$$=\tanh^{-1}\left[p_{||}/(p_{||}{}^2+p_\perp{}^2+m^2c^2)^{1/2}\right]\ ,$$

$y=\tanh^{-1}\beta$ and m is the proton mass. (It is convenient to use the rapidities $y_{||}$ and y since these add linearly in the Lorentz transformation.) Figure 4 shows the plot of $p_\perp$ against $y_{||}$ for the present Cu(γ,p) data. The points represent invariant cross sections between 3 and 10 nb/MeV^2 sr and were taken from the proton energy region between 90 and 200 MeV; this was the region over which the data were sufficiently complete to perform this analysis. The isotropic loci were obtained by fitting Eq. (2) to these points using a least squares procedure. The symmetry axis of the resulting curves is shifted from $y_{||}=0$ by the rapidity y of the emission frame. It is evident that with only three points in the angular distribution the accuracy with which one can hope to determine the symmetry axis is limited. Over the range of cross sections measured no significant variation in the value for y was seen and its mean value was $y=0.098\pm0.017$. The error estimate includes the variation in the four fits as well as the uncertainties in the measured cross sections. This quantity is related to the mass M of the particles involved in the interaction by $\tanh y=p_\gamma/(p_\gamma+Mc)$, where p_γ is the photon momentum. The value obtained corresponds to interaction of the photon with, on the average, 3.0 ± 0.6 nucleons. For comparison, a similar analysis carried out by McKeown *et al.*[29] for the Ni(π,p) data yielded the result 4.4 ± 0.5 nucleons, somewhat higher than the Cu(γ,p) result. The (γ,p) and (π,p) analyses also differ in another respect; whereas the isotropic loci are consistent with the (γ,p) data points, this was not true for the (π,p) case,[29] for which the data might suggest the presence of two distinct production mechanisms.

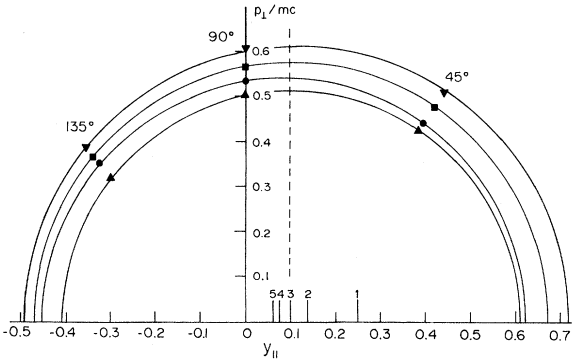

FIG. 4. Arcs representing contours of constant invariant cross section, $d^2\sigma/cp\,dE\,d\Omega$, in the range 3—10 nb/MeV^2 sr fitted to the Cu(γ,p)X data at the three angles. The data points are located by their (Lorentz invariant) perpendicular component of momentum $p_\perp$ and parallel component of rapidity $y_{||}$. The integers above the horizontal axis refer to the number of nucleons participating in the photon absorption process. The rapidity y of the symmetry axis (shown as a dashed line) determines the rapidity of the average number of participating nucleons.

It must be stressed that this analysis only gives an indication of the average number of nucleons among which the photon momentum is shared at the stage when the proton is emitted. If the protons are secondary products the initial stage may involve fewer nucleons. If, contrary to the assumption of this analysis, the proton production mechanism has an intrinsic anisotropy, then the actual number of nucleons involved could deviate in either direction from the result obtained. Since protons are probably produced by more than one mechanism, the result of this analysis represents an average value of the masses participating in these processes.

C. Comparison with inclusive (π,p) data

The resonant nature of the $A(\gamma,\pi)X$ and $A(\gamma,p)X$ total cross section[17] and of the deuteron photodisintegration cross section[30] indicates that $\Delta(1232)$ production may dominate the inclusive photoproton process at $E_\gamma=300$ MeV through real and virtual pion production processes. A calculation of the $\gamma+{}^{16}$O total cross section based on the Δ-hole formalism[31] tends to confirm this expectation by providing a reasonable description of the data.[17] Since it is well known that the pion-nucleus interaction at kinetic energies around 180 MeV is dominated by $\Delta(1232)$ production, a direct comparison between inclusive (γ,p) and (π,p) data seems appropriate. One distinguishing feature of the photon and pion probes which one hopes to exploit is the large difference between their interaction strengths.[6] Such a comparison has already been made for carbon.[32] In that case, the shapes of the averaged (π^+,p) and (π^-,p) spectra were found to be in good agreement with the (γ,p) spectra at all angles. Moreover, the magnitude of the cross sections was found to be related by a constant factor

$R[(\pi,p)/(\gamma,p)]=55\pm10$. On the basis of this evidence McKeown *et al.*[32] suggest that the protons do arise through a common mechanism, Δ production, in both reactions.

Figure 5 shows a similar comparison of the present 300-MeV Cu$(\gamma,p)X$ data and the Ni(π,p) data for $E_\pi=160$ MeV.[19] It is evident that the shapes of the corresponding spectra are again quite similar thus supporting the conclusion of Ref. 32. However, we observe in this case an angle-dependent ratio $R[(\pi,p)/(\gamma,p)]$ between the cross sections for the two reactions; the values are $R(45°)=25\pm5$, $R(90°)=30\pm5$, and $R(135°)=45\pm5$. This decrease in $R[(\pi,p)/(\gamma,p)]$ at 45° and 90° may result from the variation with angle of the final state interactions in the (π,p) reaction for a medium weight target. If the pion interacts predominantly in the "front" nuclear surface region,[5] as is suggested by the $A^{0.51}$ dependence of the total (π,p) cross section,[19] protons emitted at 45° and 90° will suffer more attenuation than at 135°. For the (γ,p) reaction, by comparison, the total cross section shows an $A^{1.1}$ dependence,[17] which indicates a more uniform interaction throughout the nucleus so that no strong angular dependence of the final state interaction is expected.

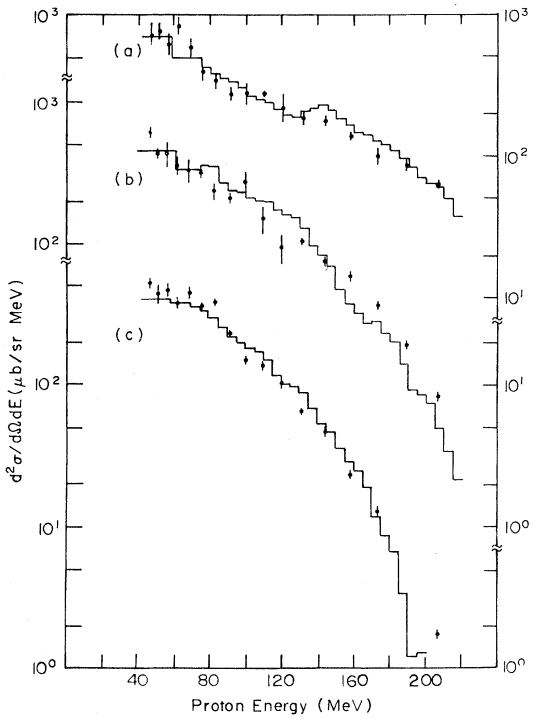

FIG. 5. Comparison of the present data for Cu$(\gamma,p)X$ at $E_\gamma=300$ MeV shown as points with charge-averaged Ni$(\pi,p)X$ data at $E_\pi=160$ MeV (Ref. 19) shown as histograms. The (γ,p) cross sections have been multiplied by a factor R which depends on the proton angle: (a) 45°, $R=25$; (b) 90°, $R=30$; (c) 135°, $R=45$.

This picture assumes that the observed protons originate from the front surface where the pion interacts. However, as Weise[33] points out, coherent multiple pion scattering, i.e., the propagation of the Δ-hole state through the nucleus, plays a large role in pion-induced reactions in the resonance region (although it is relatively unimportant in photoreactions). If the effect of this is to distribute the source of protons in the (π,p) reaction more widely through the nucleus and thus reduce the angular variation of the final state interactions, then, in principle, the comparison of proton spectra and angular distributions from (π,p) and (γ,p) reactions could provide a means of assessing the spatial propagation of the isobar in (π,p) reactions. However, to do this, Δ-hole calculations of both reactions, including their intrinsic angular distributions and final state interactions, will be necessary.

VI. CONCLUSIONS

Three simple phenomenological comparisons have been made with the data for the Cu$(\gamma,p)X$ reaction at 300 MeV presented here: (a) with an intranuclear cascade calculation; (b) with proton angular distributions calculated assuming isotropic emission from a small subgroup of nucleons, and (c) with $(\pi^\pm,p)$ data. At this rather superficial level the results are consistent with a photoreaction mechanism dominated by isobar excitation in which propagation of the isobar does not appear to play an important role although final state interactions following its decay spread the excitation energy among 3–4 nucleons. However, a thorough understanding of inclusive (γ,p) data of the type reported here requires further theoretical investigation, for example, an extension of the isobar-hole model[33–35] to cover both (γ,p) and (π,p) reactions. A detailed comparison of the proton spectra and angular distributions from both reactions with such a calculation seems to offer some prospect of information on Δ propagation in the nucleus following photon and pion absorption.

ACKNOWLEDGMENTS

This work was supported by the U. S. Department of Energy, the National Science Foundation, and the United Kingdom Science Research Council. One of us (R.S.T.) acknowledges the partial support of the Hughes Staff Doctoral Fellowship.

*Present address: Technology for Communication International, Mountain View, California 94043.
[1]J. L. Matthews *et al.*, Phys. Rev. Lett. 38, 8 (1977); D. J. S. Findlay *et al.*, Phys. Lett. 74B, 305 (1978).
[2]M. Gari and J. Hebach, Phys. Rep. 72, 1 (1981).
[3]J. T. Londergan and G. D. Nixon, Phys. Rev. C 19, 998 (1979).
[4]J. L. Matthews, *Lecture Notes in Physics, Nuclear Physics with Electromagnetic Interactions,* edited by H. Arenhövel and D. Drechsel (Springer, Berlin, 1979), p. 369.
[5]J. N. Ginocchio, Phys. Rev. C 17, 195 (1978).
[6]E. J. Moniz, in Proceedings of the June Workshop on Intermediate Energy Electromagnetic Interactions with Nuclei, Massachusetts Institute of Technology, edited by A. Bernstein, DOE Report No. COO-3069-677, 1977, p. 212.
[7]K. G. Dedrick, Phys. Rev. 100, 58 (1955). See Ref. 9 for further references.
[8]T. A. Gabriel and R. G. Alsmiller, Phys. Rev. 182, 1035 (1969).
[9]J. L. Matthews, W. Bertozzi, S. B. Kowalski, C. P. Sargent, and W. Turchinetz, Nucl. Phys. A112, 654 (1968).
[10]C. Whitehead, W. R. McMurray, M. J. Aitken, N. Middlemas, and C. H. Collie, Phys. Rev. 110, 941 (1958).
[11]J. W. Weil and B. D. McDaniel, Phys. Rev. 92, 391 (1953).
[12]R. G. Cence and B. J. Moyer, Phys. Rev. 122, 1634 (1961).
[13]P. Dougan and W. Stiefler, Z. Phys. 269, 97 (1974).
[14]G. Andersson, P. Dougan, and W. Stiefler, Z. Phys. A 272, 263 (1975).
[15]S. Homma *et al.*, Phys. Rev. Lett. 45, 706 (1980).
[16]J. Arends *et al.*, Z. Phys. A 298, 103 (1980).
[17]J. Arends *et al.*, Phys. Lett. 98B, 423 (1981).
[18]J. Arends, in *Photopion Nuclear Physics,* edited by P. Stoler (Plenum, New York, 1979), p. 275.
[19]R. D. McKeown *et al.*, Phys. Rev. C 24, 211 (1981).
[20]W. Bertozzi *et al.*, Nucl. Instrum. Methods 141, 457 (1977).
[21]E. R. Kinney, J. L. Matthews, W. W. Sapp, R. A. Schumacher, and R. O. Owens, Nucl. Instrum. Methods 185, 189 (1981).
[22]J. L. Matthews and R. O. Owens, Nucl. Instrum. Methods 111, 57 (1973).
[23]R. H. Dalitz and D. R. Yennie, Phys. Rev. 105, 1598 (1957).
[24]W. C. Barber, Phys. Rev. 111, 1642 (1958); W. C. Barber and T. Wiedling, Nucl. Phys. 18, 575 (1960).
[25]M. J. Leitch, Ph.D. thesis, MIT, 1979 (unpublished).
[26]J. Arends (private communication).
[27]T. A. Gabriel (private communication).
[28]J. N. Ginocchio and M. B. Johnson, Phys. Rev. C 21, 1056 (1980).
[29]R. D. McKeown *et al.*, Phys. Rev. Lett. 44, 1033 (1980).
[30]J. M. Laget, Nucl. Phys. A312, 265 (1978).
[31]E. Oset and W. Weise, Phys. Lett. 94B, 19 (1980).
[32]R. D. McKeown *et al.*, Phys. Rev. Lett. 45, 2015 (1980).
[33]W. Weise, Nucl. Phys. A358, 163c (1981).
[34]K. Klingenbeck, M. Dillig, and M. G. Huber, Phys. Rev. Lett. 41, 387 (1978).
[35]M. Hirata, J. H. Koch, F. Lenz, and E. J. Moniz, Ann. Phys. (N.Y.) 120, 205 (1979).